World Academy of Science, Engineering and Technology
International Journal of Mathematical and Computational Sciences
Vol:16, No:1, 2022

On Deterministic Chaos: Disclosing the Missing Mathematics from the Lorenz-Haken Equations

Belkacem Meziane

***Abstract*—**The original 3D Lorenz-Haken equations -which describe laser dynamics- are converted into 2-second-order differential equations out of which the so far missing mathematics is extracted. Leaning on high-order trigonometry, important outcomes are pulled out: A fundamental result attributes chaos to forbidden periodic solutions, inside some precisely delimited region of the control parameter space that governs self-pulsing.

***Keywords*—**Chaos, Lorenz-Haken equations, laser dynamics, nonlinearities.

I. Introduction

AMONG a variety of nonlinearly coupled differential equations to involve chaotic dynamics, the Lorenz-Haken is undoubtedly the set that implicated incomparable interest from scientists in physics and mathematics [1], [2]. Yet, at the end of the 1990's, after decades of widespread attention, Stephen Smale, the 1966 medal-Field laureate, had no other choice than include the Lorenz attractor among a list of challenging-problems for the 21st century [3]. Despite countless publications devoted to nonlinear dynamics, put out from the early 1960's to the late 1990's, Smale probes justifiably pointed out the lack of rigorous mathematical proofs to clarify the origin of aperiodic solutions. In addition, given the set of control-parameter digits that govern the dynamics of nonlinear systems, no method is put forward to predict the manifestation of chaos. The solution characteristics extract with computer algorithms.

Centered on basic trigonometry, a methodical routine applies to the coupled-oscillator model to pull out useful and genuine analytics, ultimately answering the question: Why do Lorenz-Haken equations deliver aperiodic solutions when solving with computer algorithms?

II. From the Original 3D Set to a 2-Coupled-Oscillator Model

Using Einstein's notation, the Lorenz-Haken equations, which govern laser dynamics, write [4], [5]

$$\dot{E}(t) = -\kappa(E(t) + 2CP(t)), \tag{1a}$$

$$\dot{P}(t) = -P(t) + E(t)D(t), \tag{1b}$$

$$\dot{D} = -\gamma(D(t) + 1 + E(t)P(t)) \tag{1c}$$

where $E(t)$, $P(t)$, and $D(t)$ represent, respectively, the laser field amplitude, the polarization, and the population inversion of the amplifying medium. κ and γ are the field and population relaxation rates, both scaled to the polarization decay rate, while $2C$ quantifies some external power supply, meant to break the natural thermodynamic equilibrium, and transform an initially absorbing material into an amplifier. The dot above all three variables represents the first derivative with respect to time.

In the unstable regime of operation, depending on the control parameter values, (1) delivers a wealth of solutions, accessible through computer algorithms, only. The lack of any mathematical proofs to elucidate the occurrence of chaotic dynamics led Smales [3] to hand out the strangeness of the Lorenz attractor as a challenge to the 21st century.

The present contribution aims at solving Smale problem with basic trigonometry applied to a proposed set, which consists of two second-order differential equations, derived from (1) to couple the population inversion to the electric field and laser intensity, leaving aside the medium's polarization.

The key element to the conversion method consists in reordering (1a) into

$$P(t) = -\frac{E(t)}{2C} - \frac{1}{2C}\frac{\dot{E}(t)}{\kappa} \tag{2}$$

Plugging $P(t)$ and its first derivative into (1b), we pull out a second order differential equation for the electric field, with the population inversion as the driving source

$$\ddot{E}(t) + (\kappa + 1)\dot{E}(t) + \kappa E(t) + 2C\kappa E(t)D(t) = 0 \tag{3}$$

While (1c) reorganizes, likewise, into a second order differential equation for the population inversion, as

$$\frac{1}{\gamma}\ddot{D}(t) + \dot{D}(t) + E^2(t)D(t) = \frac{1}{2C}\left(E(t)\dot{E}(t)\left(1 - \frac{1}{\kappa}\right) + \frac{\dot{E}(t)^2}{\kappa} - E(t)^2\right) \tag{4}$$

Despite their apparent complexity, compared to (1), these equations have much to offer in analytical efficiency, especially in the strong harmonic mode associated with self-pulsing and chaos.

III. Analytical Outcomes

For completeness, the two oscillators will be investigated in

B. Meziane is with the University d'Artois, Centrale Lille, ENSCL, Univ. Lille, UMR 8181 – UCCS – Unité de Catalyse et Chimie du Solide, F-62300 Lens, France (phone: 333-21-791-732; fax: 333-21-791-717; e-mail: belkacem@meziane.com).

the small and strong harmonic modes. Both modes belonging to the class of solutions the Lorenz Haken equations deliver with computer simulations.

A. The Small-Harmonic Mode

With small enough perturbations as initial conditions, the electric field and population signals consist of small amplitude oscillations around the steady state (E_0 , D_0)

$$E(t) = E_0 \ + e\cos(\omega t) \tag{5a}$$

$$D(t) = D_0 \ + dcos(\omega t) \tag{5b}$$

with $e \ll E_0$ and $d \ll D_0$. At the instability threshold, all quantities relate to the control parameters κ and γ (in the following, $\gamma = 1$ [4])

$$E_0 \ = \pm\sqrt{2C-1} = \pm\sqrt{\frac{(\kappa+1)(\kappa+2)}{\kappa-2}} \tag{5c}$$

$$D_0 \ = -\frac{1}{2C} = -\frac{\kappa-2}{\kappa(\kappa+4)} \tag{5d}$$

$$\omega = \sqrt{\frac{2\kappa(\kappa+1)}{\kappa-2}} \tag{5e}$$

Driven with (5a), (4) transforms into a series of algebraic relations pointing solutions of the form

$$D(t) = D_0 \ + d_1 \ \cos(\omega t) + d_2 \ \sin(\omega t) = D_0 \ + d\cos(\omega t - \varphi) \tag{6a}$$

yielding, with further algebra, the phase and amplitude relationships

$$\tan(\varphi) = \frac{d_2}{d_1} = \omega\left(1 - \frac{E_0^2}{\omega^2}\right) = \sqrt{\frac{(\kappa+1)(\kappa-2)}{2\kappa}} \tag{6b}$$

$$d = \frac{1}{2C}eE_0 \ \left(1 - \frac{1}{\kappa}\right) \times \frac{1}{\sqrt{1+\omega^2\left(1-\frac{E_0^2}{\omega^2}\right)^2}} = \frac{\kappa-1}{\kappa^2\ (\kappa+4)}\sqrt{\frac{2\kappa(\kappa-2)(\kappa+1)(\kappa+2)}{2\kappa+(\kappa+1)(\kappa-2)}}e \tag{6c}$$

Note the exclusive dependence on the control parameter κ.

Driven with (5b), (3) implies a solution of the form

$$E(t) = E_0 \ + e_1 \ cos(\omega t) + e_2 \ \sin(\omega t) = E_0 \ + e\cos(\omega t + \varphi) \tag{6d}$$

Additional algebra pulls out new expressions to the phase φ and amplitude e that are *identical* to (6b) and (6c).

One may conclude that, in the small amplitude regime, the electric field and population oscillators hold the same harmonic solutions, with similar phase factors and amplitude relationships, indistinctly extracting from each of the coupled oscillators. Both oscillators nonlinearly interact to deliver coherent responses with respect to one another. This constitutes a first proof to the model cogency. To explore the chaos question, we need to put attention on strong harmonic solutions. These characterize (1) when the system drives away from the permanent state (E_0 , D_0), at the onset of instability, to wander along unpredictable routes

B. The Strong-Harmonic Mode

The strong harmonic mode refers to the conditions under which the system delivers strong amplitude oscillations with zero mean values for the electric field

$$E(t) = \sum_n E_{2n+1}\cos[(2n+1)\omega t] \tag{7a}$$

While the population inversion evolves according to

$$D(t) = D_0 \ + \sum_n d_n \ \cos(2n\omega t) \tag{7b}$$

Limiting the developments to first and third order for the electric field, to second order for the population inversion, is all it takes to extract useful analytics and information. In view of their structural differences, the two oscillators are considered separately.

1. The Population Oscillator

The dominant part the driving field is its fundamental component

$$e_1 \ (t) = E_1 \ \cos(\omega t) \tag{8a}$$

injected into (4), we obtain

$$\ddot{D}(t) + \dot{D}(t) + E_1^2\frac{1+\cos(2\omega t)}{2}D(t) = \frac{1}{2C}\frac{1}{2}\left(\frac{\omega^2\ E_1^2}{\kappa} - E_1^2\right) - \frac{1}{2C}\frac{1}{2}\left(\frac{\omega^2\ E_1^2}{\kappa} + E_1^2\right)\cos(2\omega t) - \frac{1}{2C}\frac{\omega E_1^2}{2}\left(1 - \frac{1}{\kappa}\right)\sin(2\omega t) \tag{8b}$$

In response to the forcing factors, all of which contain second harmonic components, the population inversion expresses as

$$D(t) = D_0 \ + d_1 \ \cos(2\omega t) + d_2 \ \sin(2\omega t) = D_0 \ + d\cos\left(2\omega t - \varphi_2\ \right) \tag{8c}$$

Converting (4) into an algebraic equation from which gathers a series of relationships and ultimate expressions for the phase factor φ_2 and amplitude d

$$\tan\left(\varphi_2\ \right) = \frac{d_2}{d_1} = \frac{7\kappa^2\ -13\kappa+2}{9\kappa^2\ -\kappa+2}\sqrt{\frac{(\kappa+1)(\kappa-2)}{2\kappa}} \tag{8d}$$

$$d = 2\sqrt{\kappa}\frac{2(\kappa+1)(\kappa+2)}{\kappa(\kappa+4)} \times \frac{\sqrt{[2(\kappa-1)(\kappa-2)+(\kappa+1)(7\kappa-2)]^2 + \frac{(\kappa+1)(\kappa-2)}{2\kappa}[(\kappa-1)(7\kappa-2)-4\kappa]^2}}{(\kappa+1)(7\kappa-2)^2 + 8\kappa(\kappa-2)}E_1 \tag{8e}$$

Being real for any κ, these two expressions imply that driven with a strong harmonic field, the population inversion admits periodic solutions for any cavity decay rate. The same demonstration applies to any exciting higher field-order. This is not the case for the electric field oscillator, as hereafter established.

2. The Electric-Field Oscillator

Considering a driving population of the form

$$D(t) = D_0 \ + d\cos(2\omega t) \tag{9a}$$

implies a coupling factor $E(t)D(t)$ in (3), developing into first and third harmonics. The electric field response is bound to follow these same orders. Comprising essential out-of-phase components with respect to $D(t)$, $E(t)$ develops as

$$E(t) = E_1 \ \cos(\omega t) + E_2 \ \sin(\omega t) + E_3 \ \cos(3\omega t) + E_4 \ \sin(3\omega t) = E_{01}\cos(\omega t - \varphi_1\ ) + E_{03}\cos(3\omega t - \varphi_3\ ) \tag{9b}$$

With (9a) and (9b), (3) converts into somewhat lengthy but straightforward relationship, out of which extract the following equations for the first and third order amplitude ratios $\frac{E_2}{E_1}$ and $\frac{E_4}{E_3}$

$$\left[4+\frac{2C\kappa}{\omega^2}\ \frac{d}{2}\right]\left(\frac{E_2}{E_1}\right)^2 + 2\frac{2C\kappa}{\omega^2}\ \frac{d}{2}\frac{3\omega}{\kappa+1}\frac{E_2}{E_1} + 4 - \frac{2C\kappa}{\omega^2}\ \frac{d}{2} = 0 \tag{10a}$$

$$\left[4-\frac{2C\kappa}{\omega^2}\ \frac{d}{2}\right]\left(\frac{E_4}{E_3}\right)^2 + 2\frac{2C\kappa}{\omega^2}\ \frac{d}{2}\frac{3\omega}{\kappa+1}\frac{E_4}{E_3} + 4 + \frac{2C\kappa}{\omega^2}\ \frac{d}{2} = 0 \tag{10b}$$

both bearing the form of a second-degree polynomial equation $ax^2 + bx + c = 0$, with the solutions

$$\frac{E_2}{E_1} = \tan(\varphi_1\ ) = -\frac{\frac{2C\kappa}{\omega^2}\frac{3\omega\ d}{\kappa+12}}{4+\frac{2C\kappa}{\omega^2}\frac{d}{2}} \pm \frac{\sqrt{\left[\frac{2C\kappa}{\omega^2}\frac{d}{2}\frac{3\omega}{\kappa+1}\right]^2 - \left[4+\frac{2C\kappa}{\omega^2}\frac{d}{2}\right]\left[4-\frac{2C\kappa}{\omega^2}\frac{d}{2}\right]}}{\left[4+\frac{2C\kappa}{\omega^2}\frac{d}{2}\right]} \tag{10c}$$

$$\frac{E_4}{E_3} = \tan(\varphi_3\ ) = -\frac{\frac{2C\kappa}{\omega^2}\frac{3\omega\ d}{\kappa+12}}{4-\frac{2C\kappa}{\omega^2}\frac{d}{2}} \pm \frac{\sqrt{\left[\frac{2C\kappa}{\omega^2}\frac{d}{2}\frac{3\omega}{\kappa+1}\right]^2 - \left[4+\frac{2C\kappa}{\omega^2}\frac{d}{2}\right]\left[4-\frac{2C\kappa}{\omega^2}\frac{d}{2}\right]}}{\left[4+\frac{2C\kappa}{\omega^2}\frac{d}{2}\right]} \tag{10d}$$

The discriminant, which is the same in (10c) and (10d), simplifies as

$$\Delta = \left(\frac{2C\kappa}{\omega}\ \frac{d}{2}\right)^2 \left[\left(\frac{3}{\kappa+1}\right)^2 + \frac{1}{\omega^2}\right] - 16 \tag{10e}$$

Transforming, at the instability threshold, into

$$\Delta = \left(\frac{\kappa(\kappa+4)}{2(\kappa+1)}\right)^2 \left(\frac{d}{2}\right)^2 \left[\frac{18\kappa}{(\kappa+1)(\kappa-2)} + 1\right] - 16 \tag{10f}$$

Like any such polynomial equation, for real solutions to exist, $\Delta(\kappa)$ must be positive.

The discriminant, depicted Fig. 1, includes the expression for the population amplitude d (8e). The graph indicates that Δ is negative for κ values inside the range [2.17; 30.42]. The diagram may directly obtain, with minor differences, setting $d \cong 0.4$ in (10f). Consistently with (8e), the population amplitude always remains close to 0.4, for all κ's, in accordance with numerical outputs. According to this fundamental result, periodic solutions for the electric field oscillator admit exclusively outside the range of κ's with positive Δ; i.e., for $\kappa < 2.17$ and $\kappa > 30.42$. That is just about what a chart of numerical solutions indicates [4], [5]. Periodic S1 solutions are obtained with (1) for $\kappa < 2.11$ and $\kappa > 28.3$. Theoretically, inside the range [2.17; 30.42], aperiodicity and chaos should take over. These behaviors and characteristics go along computer-generated solutions, as a few typical examples demonstrate in the following section.

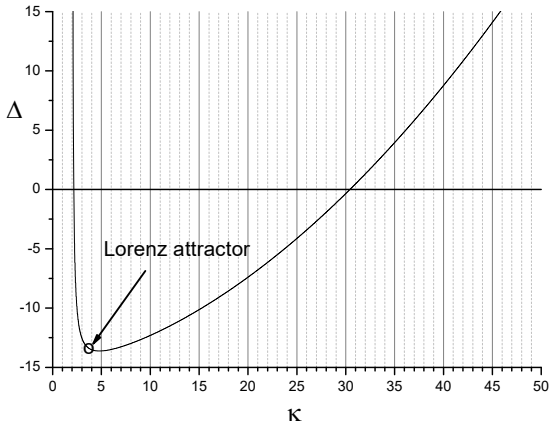

Fig. 1 Discriminant Δ vs κ, setting the limits of forbidden periodic solutions to the range [2.17; 30.42], for the electric-field oscillator

Worth mentioning is that the Lorenz attractor, pointed out with an arrow in Fig. 1, traps way down at the bottom of the graph. Such a deep position is a sign of no periodic solution to the set of parameters originally selected by Lorenz, and clears up why the corresponding trajectory designates as robust. No matter how strong the external conditions vary, the attractor keeps the same strange shape. It is easy to sense the difficulty to vary and impose conditions that would pull the system from such negative values, which imply complex amplitudes for the electric field, and make it jump to real ones, with periodic solutions. Whereas, for control-parameter-values lower than, but close to 30, the solution may always constrain to hurdle through the region of positive values and acquire the properties of an S1 orbit.

In short, in the unstable strong harmonic regime, the two coupled oscillators, derived out of the original Lorenz Haken equations, disclose no common solutions inside some specific region of the control parameter space. Whereas periodic solutions do characterize the population inversion oscillator for any κ, these are totally forbidden for the electric field oscillator inside some specifically delimited range of κ values. The following computer simulations go along these analytical properties.

IV. Analytics vs Numeric: From Computer Simulations to Analytical Solutions

The periodic and chaotic attractors represented in Fig. 2 fit-in remarkably well to the analytical graph of Fig. 1. While for $\kappa = 2.1$ (Fig. 2 (a)) the orbit is a symmetric limit cycle, it

explodes into chaotic, inside the whole range of forbidden periodic solutions. Respectively represented in Figs. 2 (b)-(d) are the attractors obtained with κ = 2.4, κ = 4.45 and κ = 16.8. Beyond κ = 30, the orbit remains permanently periodic. Conforming to the predicting mathematics are Figs. 2 (e) and (f), respectively simulated with κ = 30, and κ = 100. Indeed, it makes no sense to search for analytical portrayals of the aperiodic solutions, as those of Figs. 2 (b)-(d). On the other hand, any orbit that corresponds to control parameters values for which Δ is positive, as those of Figs. 2 (a), (e) and (f), is obtained analytically. The associated amplitudes and phase factors are extracted for the strong harmonic expressions. A few of these were developed in the preceding sections, while others are extracted with simple algebra.

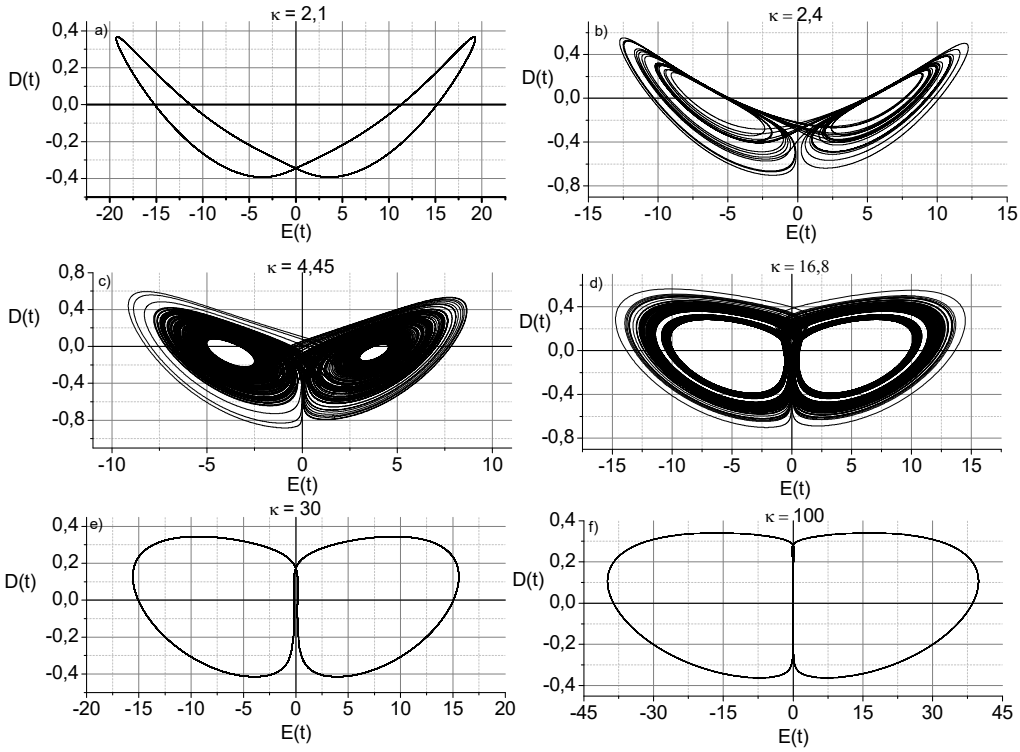

Fig. 2 Regular and chaotic orbits, numerically simulated with (1), for (a) κ = 2.1, (b) κ = 2.4, (c) κ = 4.45, (d) κ = 16.8, (e) κ = 30, and (f) κ = 100

The periodic solution, simulated with κ = 2.1, as represented in Fig. 3 (a), reproduces with the field and population expressions

$$E(t) = 19.3\cos(\omega t) \tag{11a}$$

$$D(t) = -0.01 + 0.39\cos(2\omega t + \pi/12) \tag{11b}$$

Note that in this example, the electric field third order is irrelevant. Its inclusion does not notably alter the solution.

The S1 solution of Fig. 3 (b) describes with

$$E(t) = 15.6cos^{\,3}(\omega t) \tag{12a}$$

$$D(t) = -0.03 + 0.39\cos(2\omega t + \pi/2.5) \tag{12b}$$

It corresponds to Fig. 2 (e) and κ = 30. In this case, playing some more important role, the third order harmonic cannot be neglected.

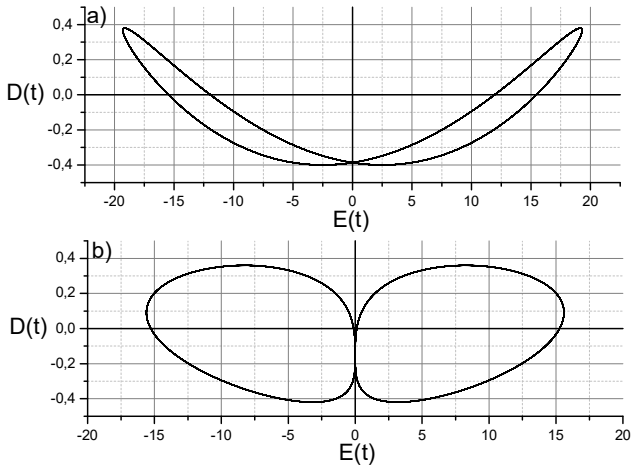

Fig. 3 Symmetric S1 phase-space orbits describing with (11) and (12). Compare with the numerical counterparts of Figs. 2 (a) and (e)

V. Conclusion

We put forward a methodical routine centered on a two-oscillator model and basic trigonometry to pull out useful and

genuine analytics, ultimately answering the question: Why do the Lorenz-Haken equations deliver aperiodic solutions when solved with computer algorithms? Our investigations clarify the question with definitive analytics, recapitulating in a clear-cut verdict: inside an accurately defined range of control parameters, the Lorenz Haken equations provide no periodic solutions.

As a straight consequence, Smale's 14th problem cracks down. The Lorenz system becoming fully decidable. Let us point out that the original set of parameters chosen by Lorenz, in his first publication, bears no specific singularity. It belongs to a widespread control parameter-range that delivers no other trajectory than aperiodic.

REFERENCES

[1] E. N. Lorenz, "Deterministic nonperiodic flow", J. Atmos. Sci. 20 1963, 130.
[2] H. Haken, "Analogy between higher instabilities in fluids and lasers", Phys. Lett. A 53, 1975, 77.
[3] S. Smale "Mathematical problems for the next century" Math. Intell. 20, 1998 7–15.
[4] B. Meziane, "Isomorphic transformation of the Lorenz equations into a single-control-parameter structure", Int. J. Eng. Res. Sci. 2, 2016, 70-8.
[5] B. Meziane, "Lorenz-Haken dynamics-analytical framework: from symmetric to asymmetric trajectories", Phys. Scr. 94, 2019, 125217.